

SAR Calculations of Novel Wearable Fractal Antenna on Metamaterial Cell for Search and Rescue Applications

Mohamed I. Ahmed^{1, *}, Mai F. Ahmed², and Abdel A. Shaalan²

Abstract—In this paper, a novel multiband wearable fractal antenna suitable for GPS, WiMax and WiFi (Bluetooth) applications is presented. This antenna is designed to operate at four resonance frequencies are 1.57, 2.7, 3.4 and 5.3 GHz. The proposed wearable antenna may be attached to human body, so the specific absorption ratio (SAR) must be calculated. Therefore, another design to reduce SAR value with a spiral metamaterial meandered in the ground plane is introduced. In addition, a wearable fractal antenna system integrated on a life jacket is also presented.

1. INTRODUCTION

Body-worn antennas have been receiving growing interest in recent years. Experience has revealed that these antennas should operate properly in the vicinity of the human body [1] and [2]. These antennas are usually used as wearable antennas, textile antennas and body-area-network (BAN) antennas [3]. Some researches are dedicating to the development of wearable antennas where these antennas must be small and light enough to be worn or carried on one's body. In addition, special attention must be paid to the specific absorption ratio (SAR), which aids in the quantitative study of power absorption issues [3] and [4].

In this paper, a wearable fractal microstrip antenna that is significantly smaller than the conventional patch antenna and operates in assigned different frequency bands in the same time is presented.

The proposed wearable antenna may be attached to life jacket to aim for finding the human body if an accident happened, so the specific absorption ratio (SAR) must be calculated and minimized as possible. Therefore, another design with a metamaterials (MTMs) structure meandered in the ground plane is proposed and included to improve SAR value to operate our design properly in the vicinity of the human body.

For natural materials, the electrical permittivity ε and magnetic permeability μ are both positive [5].

However, metamaterials or left-hand materials are man-made materials, which produce both negative permeability and permittivity of the material. It is known as double-negative material (DNG) [6].

The structure of metamaterials, which have simultaneous negative permeability and permittivity, produces negative index of refraction that bends electromagnetic waves to the same side of the normal as the incident wave, so these materials are known as left-handed materials [7], where the index of refraction of the material can be expressed as:

$$n = \sqrt{\varepsilon_r \mu_r} \quad (1)$$

Received 7 November 2016, Accepted 24 December 2016, Scheduled 17 January 2017

* Corresponding author: Mohamed I. Ahmed (miaahmed@eri.sci.eg).

¹ Microstrip Department, Electronics Research Institute, Giza, Egypt. ² Department of Electrical & Electronics Engineering, Faculty of Engineering, Zagazig University, Zagazig, Egypt.

After using the MTMs, the amount of power absorbed by the human body tissues decreases, and the SAR value also decreases to satisfy the international safety standards (FCC & ICNIPR). The SAR quantifies the power absorbed per unit mass of tissue [8]. This quantity is defined as:

$$SAR = \frac{\sigma |E|^2}{2\rho} \quad (2)$$

where σ is the electrical conductivity in Siemens per meter (S/m), ρ the mass density in kilograms per cubic meter (Kg/m^3), and E the electric field intensity vector, with magnitude in volts per meter (V/m).

In addition, there are other benefits for MTMs structure such as

- This structure can miniaturize the size of a patch antenna or other media which researchers use for its design [9].
- Sometimes, it can achieve better return loss (S_{11}) performances than a normal antenna design without metamaterial structure [10].
- The metamaterial structure can also make impact on improving the antenna directivity gain [11].

More details about the MTMs structure are given in [12] and [13].

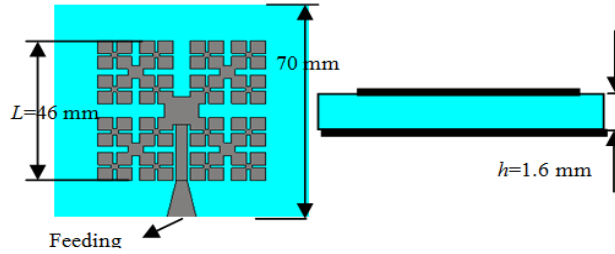


Figure 1. The antenna geometry.

2. ANTENNA DESIGN AND SIMULATION

Figure 1 illustrates the geometry of the wearable fractal microstrip antenna. A square patch is with length $L = 46$ mm, and the dimensions of the ground plane are 70×70 mm. The patch antenna and ground plane are etched on opposite sides of a substrate FR4 with thickness $h = 1.6$ mm, relative permittivity $\epsilon_r = 4.4$ and $\tan(\delta) = 0.02$. The antenna is fed by a microstrip line consisting of two parts: 50Ω line and tapered line to improve the impedance matching and achieve the best results. The optimized dimensions are mentioned in Table 1 according to Fig. 2.

Table 1. Dimensions of Stripline port.

Length	Value (mm)
W_1	3
L_1	18.4
W_2	8
L_2	12

The proposed third iteration fractal antenna is designed based on an iteration length, L_n . It is calculated as follows [14]:

$$L_n = 2L_{n+1} + W_1^{n+1} + 2W_2^{n+1} \quad (3)$$

where n is the iteration number, $W_1^{n+1} = a_1 L_n$ the width of the middle segment, and $W_2^{n+1} = a_2 L_n$ the indentation width.

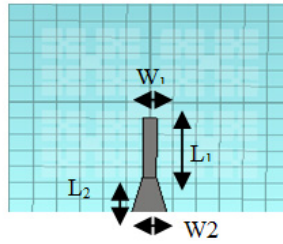


Figure 2. The port geometry.

Parameters a_1 and a_2 , which determine the efficiency of the size reduction, are ratios of middle segment width and indentation width, both with respect to the iteration length (L_n) (Hint: a_1 must be less than a_2 to avoid overlapping of elements from different iteration orders) [13]. A fractal wearable microstrip antenna presented in this paper with $a_1 = 0.1$, $a_2 = 0.4$ is deemed the most suitable for operating in assigned different frequency bands for wireless applications at the same time such as GPS, WiFi like Bluetooth, and WiMax as shown in Fig. 3.

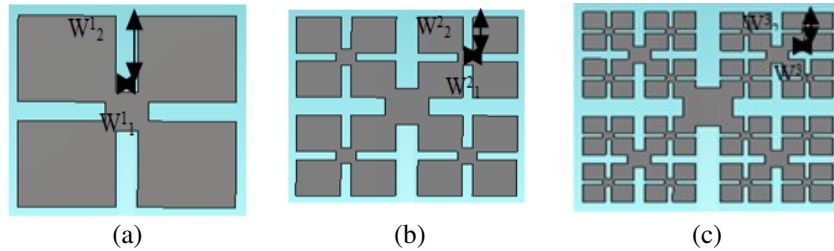


Figure 3. The wearable fractal antenna structures: (a) first iteration, (b) second iteration, and (c) proposed third iteration.

The proposed third iteration fractal wearable antenna structure is enhanced using metamaterial spiral meandered in the ground plane (as shown in Fig. 4). The permittivity, permeability, and reflection coefficient will be negative, so that the SAR value is reduced.

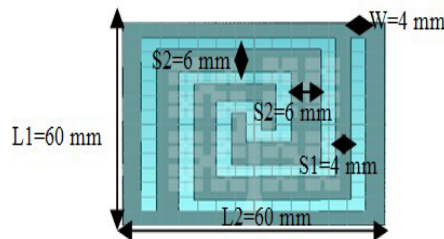


Figure 4. The spiral meandered in the ground plane.

The simulation analysis of the presented antennas is carried out by applying a commercial software package called CST 2014. The simulation of the return loss S_{11} for the conventional patch compared with the S_{11} for the first iteration, second iteration, and the proposed third iteration of the Wearable Fractal Antenna structures is shown in Fig. 5.

From the results obtained, as the order of iteration is increased, the path of the current increases so that the frequency bands from S_{11} curves shift down. We also note that the frequency bandwidths are enhanced in the proposed 3rd iteration of the wearable fractal antenna. The simulation of the return loss S_{11} for the proposed 3rd iteration Wearable Fractal Antenna (with & without) spiral meandered in the ground plane is shown in Fig. 6.

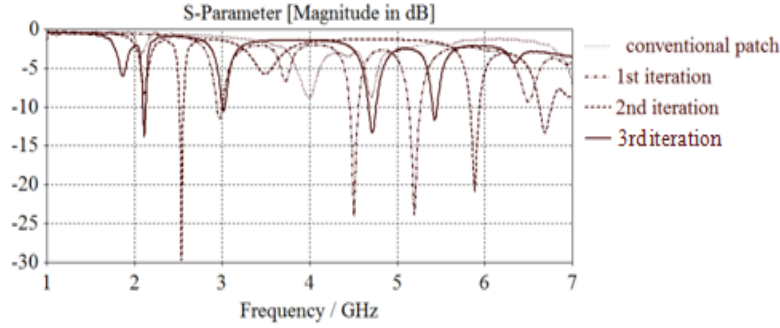


Figure 5. The return loss against frequency for 1st iteration, 2nd iteration, and the proposed 3rd iteration of the wearable antenna.

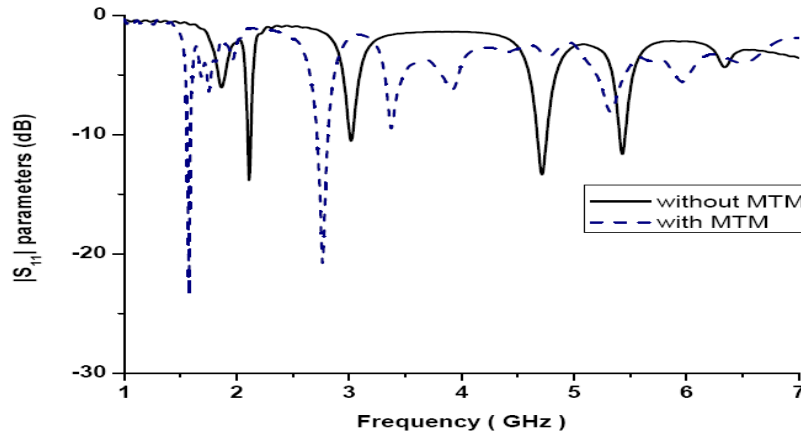


Figure 6. The return loss against frequency for the proposed 3rd iteration of the wearable antenna (with/without) metamaterials.

From Fig. 6, by comparing between the wearable fractal antennas with and without metamaterial spiral, it is found that the bandwidth is improved. Also the frequencies of the proposed antenna with MTM spiral are shifted down to operate it in assigned four different frequency bands in the same time for modern wireless applications such as GPS, WiFi and WiMax. In addition, from the results of obtaining the electrical permittivity ϵ_r and magnetic permeability μ_r for the proposed antenna with metamaterial spiral at their resonance frequencies by using a MATLAB program, which take S_{11} and S_{21} to produce the permittivity ϵ_r and permeability μ_r for this antenna, we find that they (ϵ_r and μ_r) are both negative at the intended resonance frequencies as shown in Fig. 7. So the reflection coefficient is also negative which reduces the amount of power absorbed by the human body tissue and achieves low SAR value to satisfy the international safety standards (FCC & ICNIPR). The simulation results are mentioned in Table 2.

Because the GPS antenna mainly operates with circular polarization, we calculate axial ratio curve for the proposed antenna with MTM spiral at 1.57 GHz as shown in Fig. 8.

Finally, in each resonance frequency, the current distributions are simulated as shown in Fig. 9. In addition, the radiation patterns of the proposed antennas with and without MTMs in E -plane ($\varphi = 0^\circ$) and H -plane ($\varphi = 90^\circ$) are also simulated and plotted in Fig. 10 and Fig. 11.

From Table 2, increasing the bandwidth and improving the matching at the resonance frequencies are noticed, and the electrical permittivity ϵ and magnetic permeability μ , in all the frequency bands, are both negative which reduces the amount of power absorbed by the human body tissue. In addition, the gains and radiation efficiencies of the proposed antenna with metamaterial spiral are increased, so, the antenna performance is improved.

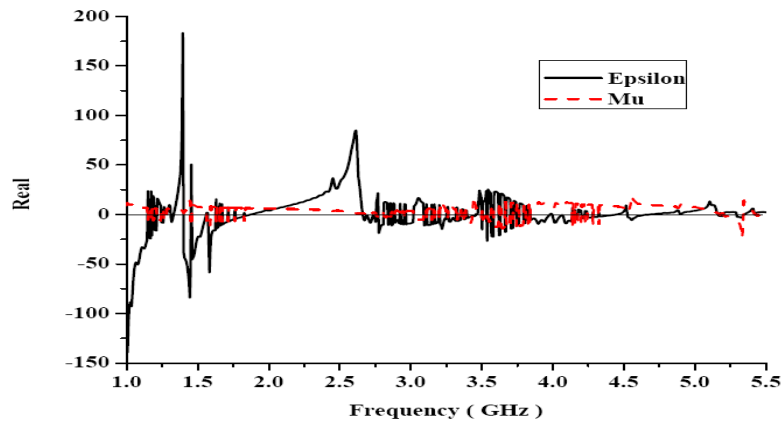


Figure 7. The electrical permittivity ϵ_r and the magnetic permeability μ_r against frequency from Matlab program.

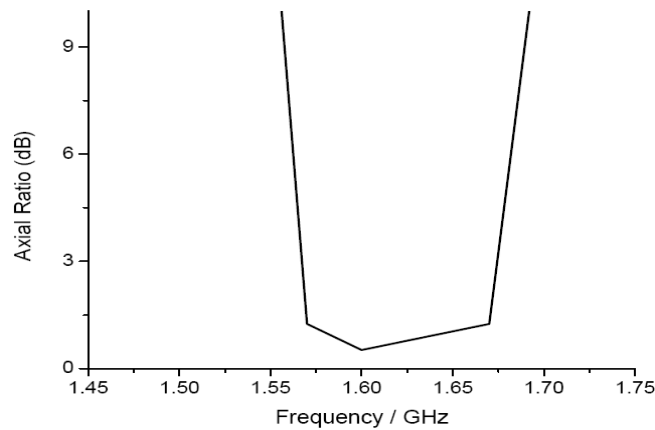


Figure 8. The axial ratio against frequency for the proposed antenna with MTM spiral meandered in the ground plane.

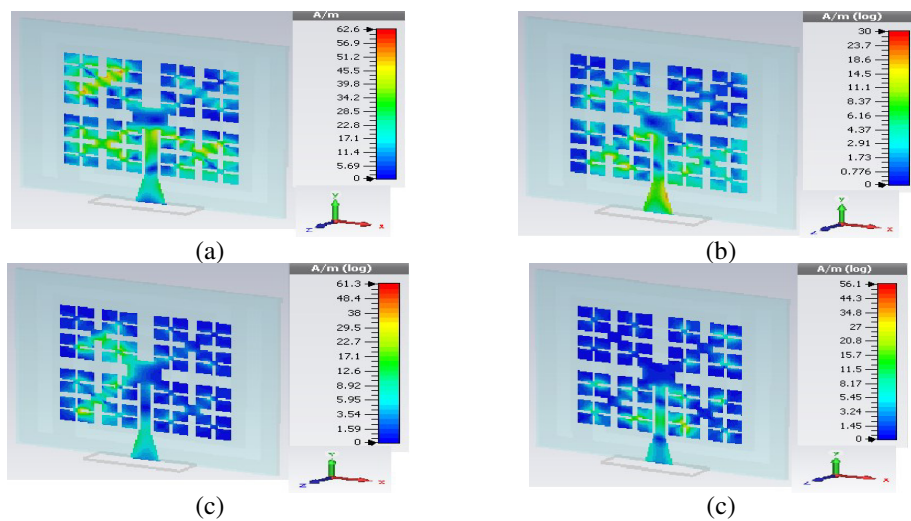
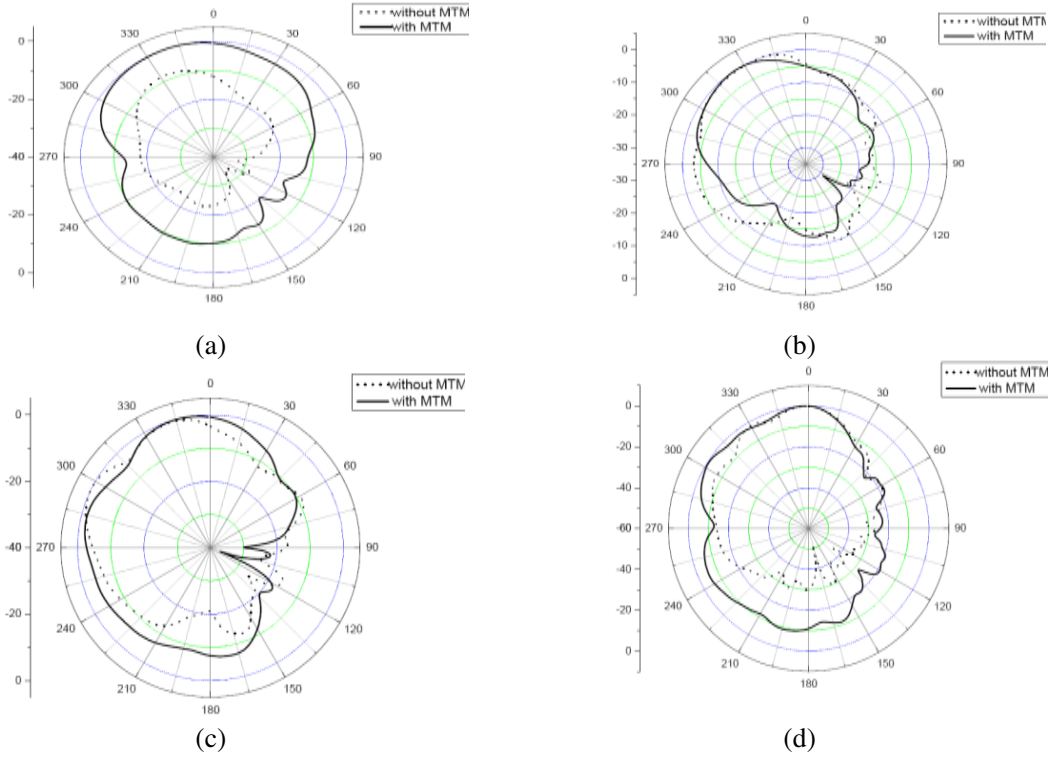


Figure 9. The current distribution for the proposed 3rd iteration of the wearable fractal antenna with MTMs at (a) 1.57 GHz, (b) 2.7 GHz, (c) 3.4 GHz and (d) 5.3 GHz.

Table 2. The simulation results of the proposed wearable fractal antenna with/without metamaterials.

Resonant Frequency Bands (GHz)		1.54–1.62	2.67–2.87	3.33–3.46	5.24–5.42
Return Loss S_{11} (dB)		-23.54	-20.78	-9.67	-8.56
Epsilon (ϵ_r)		-14.17	-18.68	-6.61	-0.49
Mu (μ_r)		-7.61	-2.51	-7.23	-22.65
without MTMs	Gain (scalar)	0.152	0.19	0.112	1.29
	Efficiency (%)	24.7	27.2	16.6	38.5
with MTM	Gain (scalar)	1.41	3.56	1.8	2.38
	Efficiency (%)	39.1	40.54	37.45	48.1
Applications		GPS	WiMax	WiMax	WiFi

**Figure 10.** The radiation pattern for the proposed 3rd iteration of the wearable fractal antenna with/without MTMs in E -plane ($\varphi = 0^\circ$) at (a) 1.57 GHz, (b) 2.7 GHz, (c) 3.4 GHz and (d) 5.3 GHz.

3. EXPERIMENTAL RESULTS AND DISCUSSION

To verify the conclusions drawn from the simulation, two microstrip antennas were fabricated on FR4 substrates by photolithography. The permittivity of the substrate is 4.4, the substrate thickness 1.6 mm, and $\tan \delta = 0.02$. The measurement results were obtained using Agilent8719ES VNA. The fabricated proposed antenna without spiral MTMs is shown in Fig. 12(a) and the simulated and measured S_{11} for that antenna are plotted in Fig. 12(b). The fabricated proposed antenna with spiral MTMs meandered in the ground plane is shown in Fig. 13, and the simulated and measured S_{11} for this antenna are plotted in Fig. 14. From these results, it is found that the measured results agree well with the simulated ones.

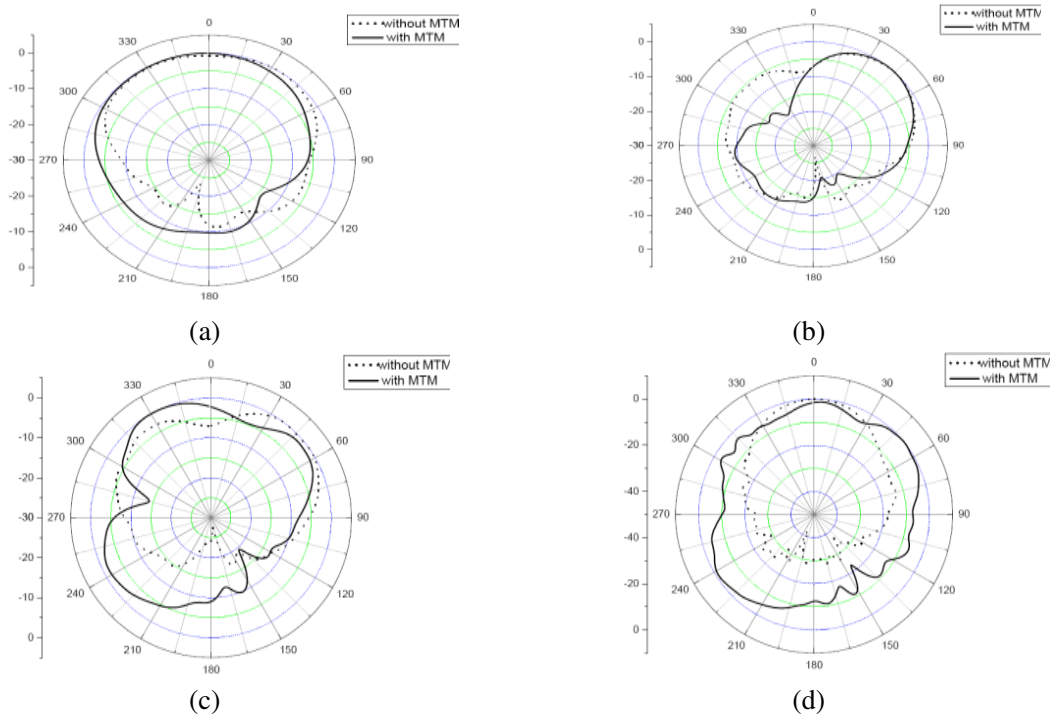


Figure 11. The radiation pattern for the proposed 3rd iteration of the wearable fractal antenna with/without MTMs in H -plane ($\Phi = 90^\circ$) at (a) 1.57 GHz, (b) 2.7 GHz, (c) 3.4 GHz and (d) 5.3 GHz.

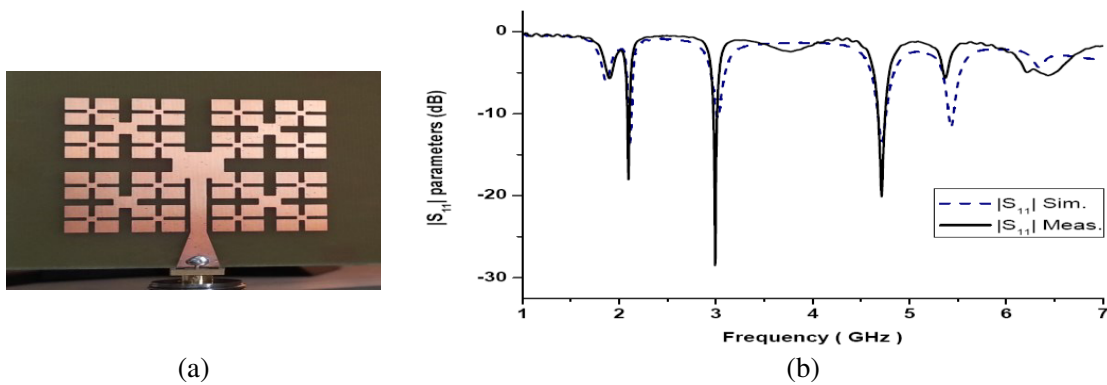


Figure 12. The fabricated proposed antenna without MTMs: (a) fabricated geometry, and (b) the measured and simulated return loss S_{11} with the freq.

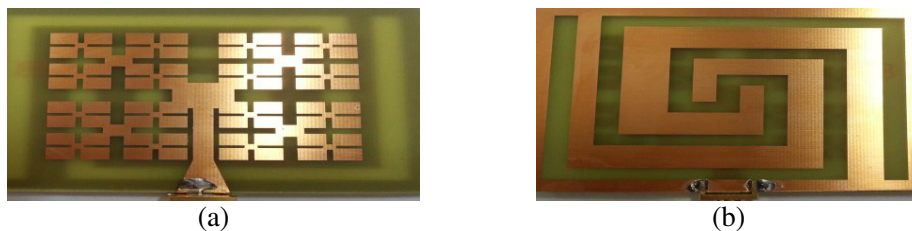


Figure 13. The fabricated proposed antenna with MTMs (a) top and (b) bottom view.

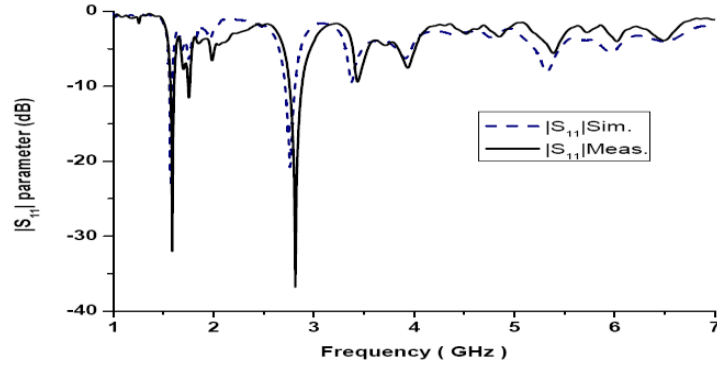


Figure 14. The measured and simulated return loss S_{11} with the freq. for fabricated proposed antenna with MTMs.

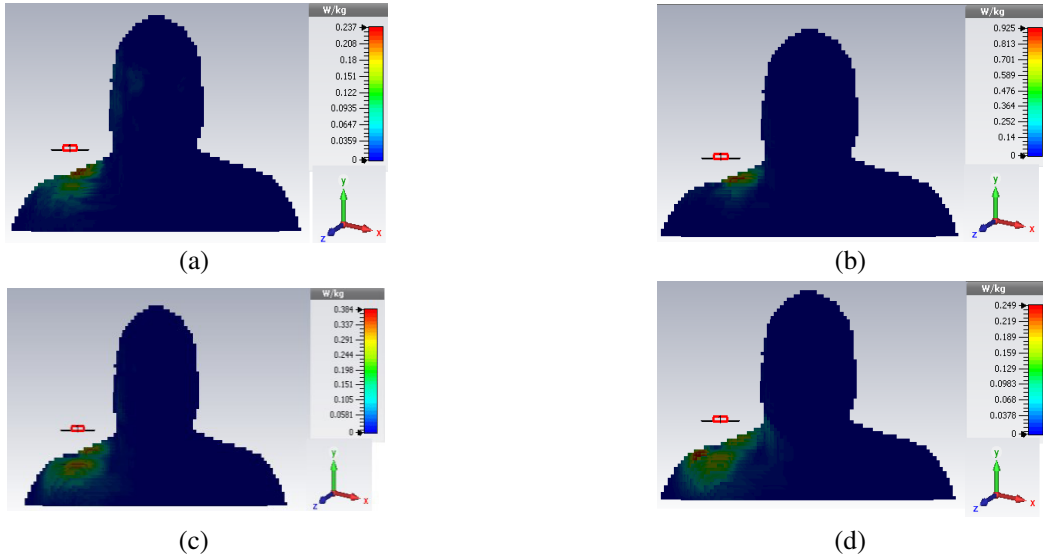


Figure 15. SAR distribution on human voxel model (10g) in distance 10 mm from antenna at (a) 1.57 GHz, (b) 2.7 GHz, (c) 3.4 GHz and (d) 5.3 GHz.

4. SAR CALCULATIONS

Figure 15 shows that the SAR simulation results for the proposed antenna with spiral MTMs, and these results are shown in Table 3 and Table 4.

From Table 3 and Table 4, the low SAR value at all the resonance frequencies is noticed to satisfy

Table 3. The max. average SAR values for the proposed antenna in various distance changes from 10 mm to 50 mm by the standard the FCC ($SAR < 1.6 \text{ mW/kg}$) (1g).

Resonance Frequency (GHz)	SAR(W/kg)				
	10 mm	20 mm	30 mm	40 mm	50 mm
1.57	0.452	0.321	0.241	0.1914	0.155
2.7	1.1	1.02	0.898	0.786	0.662
3.4	0.67	0.532	0.398	0.294	0.218
5.3	0.75	0.5318	0.407	0.303	0.278

Table 4. The max. average SAR values for the proposed antenna in various distance changes from 10 mm to 50 mm by the standard the ICNIRP (SAR < 2 mW/kg) (10 g).

Resonance Frequency (GHz)	SAR (W/kg)				
	10 mm	20 mm	30 mm	40 mm	50 mm
1.57	0.237	0.172	0.131	0.105	0.086
2.7	0.925	0.769	0.622	0.467	0.356
3.4	0.384	0.298	0.22	0.166	0.133
5.3	0.249	0.195	0.151	0.115	0.121

the international safety standards (FCC & ICNIPR) (1 g & 10 g).

When the distance between the antenna and the human model is increased, the SAR value is decreased. In addition, we note that all the SAR value results do not exceed unity. Therefore, the proposed 3rd iteration of the fractal wearable antenna with metamaterial spiral has a very low SAR value.

A wearable fractal antenna system integrated on a life jacket is also presented where this antenna may be attached to life jacket to help in finding the human body if an accident happens. The life jacket can also be considered as an isolation cover to protect the proposed antenna from the water, so the water resistance for this antenna will increase [15].

With the life jacket shown in Fig. 16, we intend to simulate it as an isolating and floating box consisting of three layers: rubber, air, rubber shown in Fig. 17, and the dimensions and electrical characteristics of its box are shown in Table 5.



Figure 16. Typical floating life jacke.

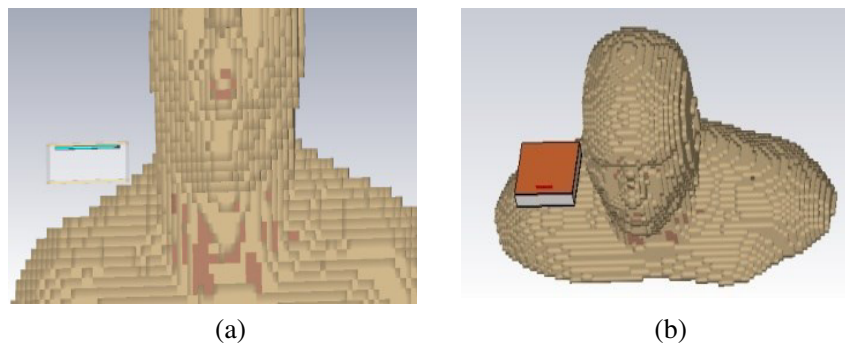


Figure 17. The possible antenna placement attached to simulated life jacket: (a) front view, and (b) top view.

Table 5. The dimensions and some of electrical characteristics for the simulated life jacket.

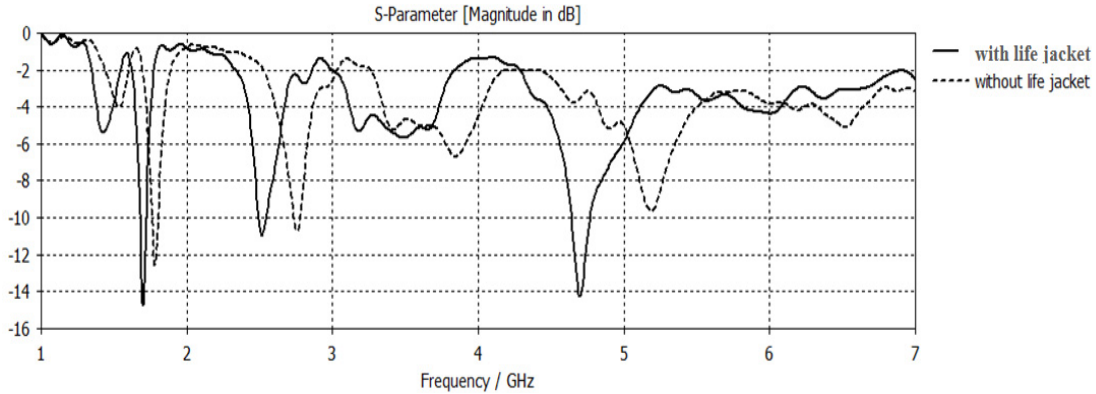
Layer Type	Layer Thickness (mm)	Dielectric constant (ϵ_r)	Tangent Loss σ
Rubber	1.9	3	0.0025
Air	20	1	0.002

The reflection coefficients for the proposed antenna with and without the life jacket are shown in Fig. 18. In addition, the gain and radiation efficiency results for this antenna with the simulated life jacket are shown in Table 6.

Table 6. The simulation results of the proposed Wearable fractal Antenna with life jacket.

Resonance Frequency (GHz)	Gain (dB)	Rad. Efficiency %
1.57	1.11	37.3
2.7	2.89	41.2
3.4	1.65	42.3
5.3	2.42	33.4

As can be observed from Fig. 18, the antenna is slightly detuned and the reflection coefficient minimum shifted toward lower frequencies. Nonetheless, the bandwidth requirement is still fully satisfied.

**Figure 18.** The return loss against frequency for the proposed antenna with and without life jacket.**Table 7.** The max. average SAR values for the proposed antenna with the simulated life jacket by the standard FCC ($\text{SAR} < 1.6 \text{ mW/kg}$) (1 g) and the standard ICNIRP ($\text{SAR} < 2 \text{ mW/kg}$) (10 g).

Resonance Frequency (GHz)	SAR (W/kg)	
	1 g	10 g
1.57	0.232	0.125
2.7	0.607	0.314
3.4	0.632	0.529
5.3	0.347	0.147

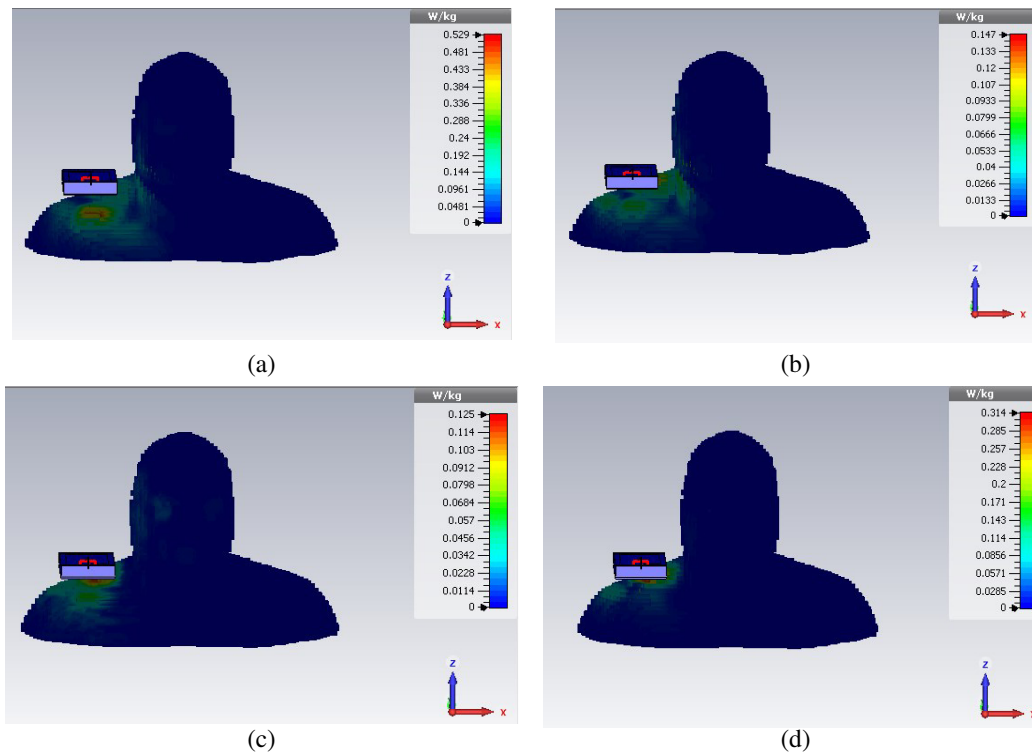


Figure 19. SAR distribution on human voxel model (10 g) in distance 10 mm from antenna with the simulated life jacket at (a) 1.57 GHz, (b) 2.7 GHz, (c) 3.4 GHz and (d) 5.3 GHz

Comparing between Table 2 and Table 6, it is found that the gain and radiation efficiency are slightly decreased due to the existence of the life jacket. But this antenna still shows acceptable performance when the life jacket is worn by a user. In addition, the SAR value is improved as shown in Fig. 19 and the rubber considered as a waterproof material which prevents the water to reach the proposed antenna. The SAR simulation results are shown in Table 7.

5. CONCLUSION

A novel wearable fractal antenna suitable for GPS, WIMAX and WIFI (Bluetooth) applications at the same time is designed and fabricated. This antenna comprises 3rd iteration fractal patch and microstrip line feed consisting of two parts: strip line plus tapered to achieve the best impedance matching and improve the antenna performance. Because this antenna is a wearable antenna and attached to human body, the specific absorption ratio (SAR) is considered an important parameter and must be calculated and improved. Therefore, another design is introduced and fabricated to enhance the SAR value, which has a spiral MTM meandered in the ground plane producing negative electrical permittivity ϵ_r and magnetic permeability μ_r . Therefore, the SAR will decrease, and the amount of power absorbed by the human body tissue will also decrease. Finally, our design is operated properly in the vicinity of the human body. In addition, a wearable fractal antenna system to be integrated on a life jacket is presented. This antenna makes the life jacket as a smart jacket to aid for finding the human body if an accident happens.

REFERENCES

1. Ahmed, M. I., E. A. Abdallah, and H. M. Elhennawy, "Novel wearable eagle shape microstrip antenna array with mutual coupling reduction," *Progress In Electromagnetics Research B*, Vol. 62, 87–103, 2015.

2. Nepa, P. and H. Rogier, "Wearable antennas for off-body radio links at VHF and UHF band," *IEEE Antennas & Propagation Magazine*, Vol. 15, 1045–9243, October 2015.
3. Ahmed, M. I., E. A. Abdallah, and H. M. Elhennawy, "SAR investigation of novel wearable reduced-coupling microstrip antenna array," *International Journal of Engineering and Technology-IJENS*, Vol. 15, No. 3, 78–87, June 2015.
4. Ismail, M., H. Elsadek, E. A. Abdallah, and A. A. Ammar, "Modified pulse 2.45 fractal microstrip patch antenna," *Wseas Transactions on Communications Journal*, Vol. 7, 280–288, ISSN: 1109-2742, April 2008.
5. Ishimaru, A., *Electromagnetic Wave Propagation, Radiation and Scattering*, Prentice Hall, 1991.
6. Nornikman, H., B. H. Ahmed, M. Z. A. Abd Aziz, and A. R. Othman, "Effect of single complimentary split ring resonator structure on microstrip antenna design," *IEEE Symposium on Wireless Technology and Application (ISWTA)*, Indonesia, September 2012.
7. Varadan, V., "Radar absorbing applications of metamaterials," *Region 5 Technical Conference, IEEE*, 10–108, 2007.
8. IEEE C95.1-2005, "IEEE standards for safety levels with respect to human exposure to radio frequency electromagnetic fields, 3 KHz to 300 KHz," Institute of Electrical and Electronics Engineers, New York, NY, 2005.
9. Zani, M. Z. M., M. H. Jusoh, A. A. Sulaiman, N. H. Baba, R. A. Awang, and M. F. Ain, "Circular patch antenna on metamaterial, electronic devices," *International Conference on Systems and Applications (ICEDSA)*, 313–316, 2010.
10. Gummalla, A., C. J. Lee, M. Achour, "Compact metamaterial quad-band antenna for mobile application," *International Symposium on Antennas and Propagation Society*, 1–4, 2008.
11. Feresidis, A. and J. C. Vardaxoglou, "Flat plate millimeter wave antenna based on partially reflective FSS," *International Conference of Antenna and Propagation*, Vol. 1, 33–36, 2001.
12. Engheta, N. and R. W. Ziolkowski, "Introduction, history, and selected topics in fundamental theories of metamaterials," *Metamaterials: Physics and Engineering Explorations*, 17–19, IEEE Explore Digital Library (2010), (Books — Metamaterials section), Retrieved 2010-05-01, John Wiley & Sons, Inc., 2006.
13. Abdalla, M. A. and Z. Hu, "Compact metamaterial coplanar waveguide ferrite tunable resonator," *IEEE, IET Microwaves, Antennas & Propagation*, 406–412, 2016.
14. Ismail, M., H. Elsadek, E. A. Abdallah, and A. A. Ammar, "New configurations of planar fractal microstrip antenna," *IEEE International Symposium on Antennas and Propagation*, San Diego, California, July 5–12, 2008.
15. Serra, A. A., P. Nepa, and G. Manara, "A wearable two-antenna system on a life jacket for Cospas-Sarsat personal locator beacons," *IEEE Trans. Antennas Propag.*, Vol. 60, No. 2, 1035–1042, February 2012.